Path planning for LiDAR equipped UGV considering coverage and efficiency in building inspection

Yun Cao[1], Ying Lo[1] and Cheng Zhang[1]

[1]Department of Civil Engineering, Design School, Xi'an Jiaotong-Liverpool University, Suzhou, China
yun.cao23@student.xjtlu.edu.cn y.lo18@student.xjtlu.edu.cn cheng.zhang@xjtlu.edu.cn

Abstract –

Construction quality inspection plays a crucial role in ensuring safety and quality at all stages of a project. However, traditional quality inspection has certain limitations, such as time consuming, expensive equipment, and cumbersome processes. Therefore, improving inspection technologies and processes by utilizing Unmanned Ground Vehicle (UGV) equipped with relatively low-cost LiDAR to enhance data collection coverage and efficiency during inspections has become a pressing issue in current construction quality management.

The main objective of this paper is to explore methods for enhancing the data acquisition capabilities of UGV equipped with low-cost LiDAR in construction environments and to experimentally verify the impact of path planning methods on data accuracy. The research focuses on investigating a new algorithm that simulates LiDAR scanning by UGV in point cloud space through 3D modeling and iteratively selects paths using Genetic Algorithm (GA) to preserve the path with the highest point cloud data collection efficiency. The experimental results extract the coordinates of the selected paths based on different scenarios, providing data support for the application of UGV on construction sites and promoting the adoption of intelligent building inspection methods.

Keywords –

Building Inspection; Unmanned Ground Vehicles; Path Planning

1 Introduction

Building inspections are critical to ensuring construction safety and engineering quality within the built environment. This process not only directly affects the structural stability of buildings but also effectively reduces safety hazards during construction, thereby safeguarding lives and property [1]. However, traditional building inspection methods, such as supervisory inspections, third-party testing, self-inspection, and non-destructive testing techniques, still face numerous limitations in practical applications. These limitations include lengthy inspection cycles, cumbersome and complex equipment, and subjective evaluation results that lack consistency and comprehensiveness [2,3]. Furthermore, these methods are constrained by technological means and inspection scope, making it difficult to adequately address potential issues during construction, thereby limiting their applicability in complex construction environments. These shortcomings may adversely impact construction progress to some extent. Therefore, optimizing inspection technologies and processes to improve the efficiency and accuracy of building quality inspections has become an urgent issue in the field of construction quality management [4].

Today, the development of building quality inspection technologies demonstrates a significant trend toward informatization, intelligence, and automation [5]. The use of robots for detecting and monitoring construction environments has gradually become a research hotspot [1]. Their application plays a critical role in reducing human error and improving the efficiency of inspection tasks. Common unmanned platforms include UGV, which exhibit significant payload and functional advantages, enabling them to carry larger-scale inspection equipment [6]. This includes cameras for visual data collection, LiDAR and laser scanners for 3D data acquisition, ground-penetrating radar (GPR) for behind-wall and underground detection, as well as components like inertial measurement units (IMUs) with ultra-wideband (UWB) sensors and global positioning systems (GPS) [7], which play an essential role in positioning and navigation. Among these, LiDAR, with its exceptional ranging accuracy and reliability, has become an essential tool in the architecture, engineering, and construction (AEC) industry, showing promising applications in environmental modeling and mapping [8]. Specifically, comparing the dimensions, positions, and orientations of building components detected on-site with the design parameters in Building Information Modeling (BIM) can effectively identify discrepancies with the BIM model [9].

However, the noisy construction environment significantly interferes with LiDAR scanning, making it a key challenge to achieve high-quality point cloud data acquisition in complex and cluttered environments [10]. Recent research has mainly focused on optimizing trajectory planning for unmanned platforms to enable efficient and high-precision data acquisition. These methods take into account factors such as energy efficiency, planning time, data redundancy reduction, and adaptability. They aim to address challenges such as minimizing energy consumption, reducing travel time, and maximizing data collection efficiency [11]-[13]. However, research focusing on solving path planning problems through path optimization algorithms to enhance data collection coverage remains relatively limited. This limitation constrains the depth and scope of theoretical advancements in this field.

2 Literature review

In order to achieve efficient environmental perception and navigation, path planning algorithms play a crucial role in this process. Traditional path planning algorithms are categorized into cell decomposition methods, roadmap-based methods, graph search-based path planning methods, and sampling-based path planning algorithms [14]. In both cell decomposition and roadmap methods, the shortest path between the starting and target positions is often determined using graph search algorithms. Graph-based path planning methods typically rely on environmental maps as prior input information, making them suitable for static planning scenarios. Among these, Dijkstra's algorithm is one of the most well-known graph traversal search algorithms, designed to find the shortest path between two nodes in a graph [15]. However, when the search space is large, the computation time of Dijkstra algorithm increases significantly. To address this, Peter E. Hart proposed the A* algorithm based on Dijkstra algorithm [16]. As a heuristic search method, A* is widely used in path planning for autonomous driving and robotics. By introducing a heuristic approach to guide the search towards the target node, A* effectively reduces the number of graph nodes explored, thus accelerating the search process. Through comparison with Figure 1, it is evident that the A* algorithm reduces the computational load compared to the Dijkstra algorithm.

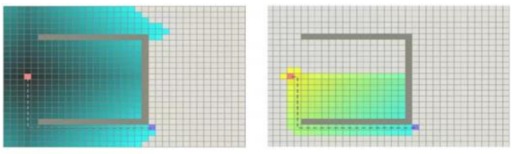

Dijkstra A*

Figure 1. Comparison of A* and Dijkstra [16]

In addition, to adapt path planning algorithms to different application requirements (such as dynamic planning, variable target nodes, and path angles) [17], improving computational efficiency is crucial. The A* algorithm performs exceptionally well in this regard, making it particularly advantageous in static environments [16]. In recent years, researchers have worked on improving the A* algorithm to overcome its limitations.Wang et al. proposed an enhanced version of the A* algorithm that takes into account vehicle contour, speed, and dynamics constraints, thereby providing safer and smoother path planning for self-driving cars [18]. Bao et al. introduced a dynamic weight-adjusted 16-way search method that reduces redundant search nodes, thus improving path planning efficiency. These improvements aim to optimize path lengths, reduce turn times, and improve overall performance [19]. Although the A* algorithm still faces many challenges in practical applications, it is applicable to more and more application scenarios as researchers continue to improve it, and still plays an indispensable role in path planning.

However, most of the research on path planning algorithms is used to perform path navigation, obstacle avoidance, etc. Nguyenet al. proposed a new path planning algorithm, NSPMR (Near-Shortest Path for Mobile Robot), based on the improvement of the traditional local path planning algorithm [20]. It is specifically designed to solve the path optimization and obstacle avoidance problem for mobile robots (MRs) when navigating in known or unknown environments. The algorithm generates an approximate shortest path by integrating sensor data in real time, which effectively avoids the limitations of traditional algorithms in the problems of “local minima” and “infinite loop”.Dong et al. proposed a combination of the optimized A* algorithm and the dynamic window algorithm to optimize the path of a mobile robot in a known or unknown environment [21]. A* algorithm and Dynamic Window Algorithm (DWA) to solve the global optimization and dynamic obstacle avoidance problems in path planning for automated guided vehicles (AGVs) [21]. The optimized A* algorithm improves the traditional algorithm's deficiencies in path smoothness and computational efficiency by means of adaptive heuristic functions and redundant point deletion, and is capable of achieving globally optimal path planning in static environments. Baras et al. proposed a Covered Path Planning (CPP) optimization method for UGV to conserve energy with a focus on Reducing the number of UGV turns through area allocation, and significantly improving the energy utilization through path optimization [22]. In the paper, the environment is partitioned and the boundaries are finely adjusted to reduce the region mixing phenomenon, while the node exchange mechanism is introduced to optimize the generated coverage paths, thus reducing the number of path turns and energy consumption. Experimental results show that the method outperforms traditional algorithms, such as A*-DARP+STC, in different obstacle ratios and complex terrains, and exhibits significant advantages in terms of the number of turns and energy efficiency. The study provides a more efficient solution for path planning of multi-UGV tasks and lays a theoretical foundation for energy-aware path planning in dynamic environments.

These studies typically emphasize minimizing path length and ensuring driving safety, often overlooking the specific requirements for scan coverage and data collection accuracy in construction sites. As a result, the adaptability of existing path optimization algorithms in construction environments remains insufficient. The main difference between this study and previous BIM-based robot path planning methods is that our approach is specifically designed to address the issue of data loss often encountered by unmanned vehicles during point cloud collection due to the noisy construction site environment. The goal is to simulate the collaboration between UGV and LiDAR and optimize the path through algorithmic iterations until the path that allows the UGV to collect the most complete point cloud model is obtained, along with its corresponding path coordinates.

3 Methodology

The method of this study aims to improve the coverage and efficiency of 3D point cloud data collection using unmanned platforms equipped with LiDAR sensors. As shown in Figure 2, the process begins with LiDAR accuracy assessment, where the impact of path planning methods on point cloud accuracy is validated. The next stage is path planning via algorithm, which consists of two parts: algorithm execution and model preprocessing. Preprocessing includes converting the BIM model into a point cloud model and adjusting the coordinate system to ensure data alignment and analysis.

After preprocessing, the feasible path for the UGV is first generated using the A* algorithm. Then, the path points undergo crossover mutation, and the GA is executed to generate the path with the highest number of collected point cloud points, the data processing stage begins, where the path length and point cloud quantity are standardized, unifying the units of path length and point cloud quantity to facilitate scoring and selecting the optimal path required for the experiment. Finally, the path is evaluated using a scoring mechanism to select the final optimized path.

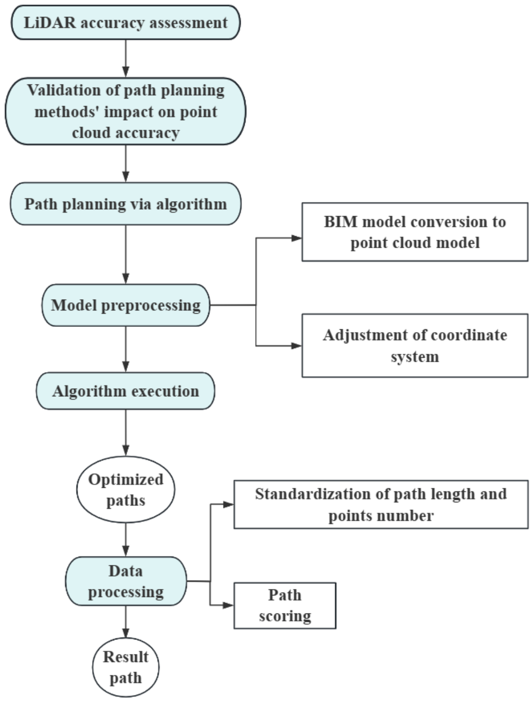

Figure 2. Proposed methodology

To verify the impact of path planning methods on the accuracy of point cloud data, experiments were conducted in both structured and unstructured scenarios (as shown in Figure 3). The experiment in the structured scene was conducted to obtain the accuracy of the UGV when scanning with the mounted LiDAR. Point cloud data was collected along different path types (2 meters, 4 meters, 6 meters, and 8 meters) using both an UGV and a Terrestrial Laser Scanner (TLS), with the high-precision point cloud data collected by the TLS serving as the baseline. After denoising, the dimensions of the target point clouds collected by the two devices were calculated using the C2C (cloud-to-cloud distance) method to ultimately obtain the scanning accuracy results.

Based on the experimental results from the structured scenario, the optimal path for UGV data collection was planned in the unstructured scenario, which simulates the construction site environment where the UGV operates in practical applications, and point cloud data was collected along both the planned path and random paths. Data processing in the unstructured scenario also included noise removal and denoising, but further comparisons of the scanning accuracy for different path types were made to verify the effectiveness of path planning methods in improving UGV scanning accuracy in complex environments.

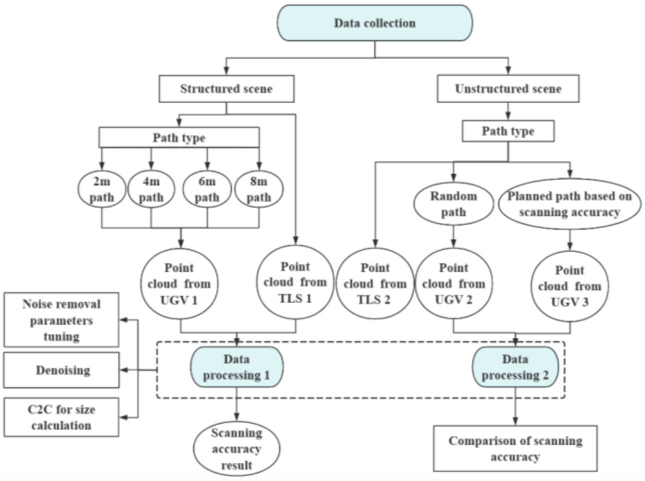

Figure 3. Experimental Workflow for verifying path planning impact on scanning accuracy

4 Case study

4.1 Theoretical verification phase

4.1.1 Mid360 precision exploration

According to existing studies, Lo et al. analyzed the data collection capability of a UGV equipped with the Mid360 in a structured scenario, with the data evaluated using the Level of Accuracy (LoA) rating. The results showed that at a distance of 2 meters, the measurement accuracy was the highest, with errors close to the sub-centimeter level, reaching an LoA30 rating, and the noise was almost negligible. In contrast, when the measurement distance increased to 8 meters, the measurement accuracy significantly decreased, with higher noise intensity and greater measurement errors, approaching 2 centimeters, and the rating dropped to LoA20. This indicates that as the measurement distance increases, the accuracy of LiDAR data is significantly affected. Additionally, at measurement distances of 2 meters and 4 meters, some point cloud data for the cardboard box were lost (as shown in Figure 4) [23].

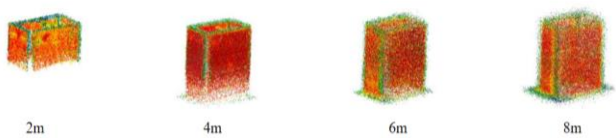

Figure 4. Point cloud modeling for different distance conditions [23]

4.1.2 Data collection in unstructured scene

In the Civil Engineering Laboratory at university, the researchers selected a structural column as the target to evaluate the effectiveness of using a path planning method to enhance the point cloud data collection capability of an UGV equipped with the Livox Mid360 in an unstructured scenario. As shown in Figure 5, a closed-loop route was laid out with yellow tape in the underground laboratory (at a distance of 4-6 meters from the target column), the path of the UGV shown in Figure 6. To control variables (data collection time), the UGV in this experiment maintained the same speed (0.6 m/s) and performed multiple data collections along both the planned path and random paths. A set of data files with similar file sizes was selected for accuracy comparison.

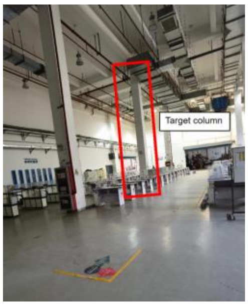

Figure 5. Column target in unstructured scene

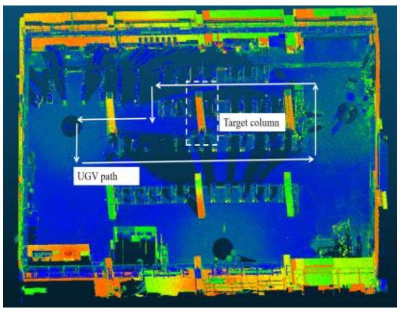

Figure 6. UGV path in unstructured scene

4.1.3 Data analysis in unstructured scenes

Table 1. Point cloud accuracy results for different paths

		TLS	Standard Deviation	UGV(2)	Standard Deviation	Error	UGV(3)	Standard Deviation	Error
Concrete	Width	0.608	0.0037	0.651	0.009	0.037	0.574	0.0151	0.032
Column	Length	0.613		0.627		0.046	0.578		0.035

The denoising process first requires separating the point cloud data of the target column collected by the TLS and UGV (with TLS data serving as the baseline) and measuring its width and length. The measurement results are shown in Table 1. It is worth noting that although the standard deviations are similar, the error range of the Livox Mid360 is slightly larger than the results of the 4m to 6m control distance experiment. This indicates that noisy environments can affect the accuracy of LiDAR data.

The point cloud data collected by the UGV shows slightly higher accuracy in path planning, but both datasets fall within the LoA20 class (Height measurements were not taken into account due to obstructions caused by the mechanical, electrical, and plumbing (MEP) systems on the ceiling). Furthermore, in the point cloud model collected along the random path, the length and width of the near-square target column were recorded as 0.651m and 0.627m, respectively, with an error of 0.24m. In summary, the data error collected by the UGV along the prescribed path was smaller than that collected along the random path.

4.2 Path planning phase

Building on this previous work, this section explores how to optimize path planning through algorithms. The focus of the research is on the global path planning problem for UGV in static environments, aiming to design a path that collects the most point clouds. During the path planning process, it is crucial to consider obstacles and danger zones in the environment, ensuring the path avoids impassable obstacles. At the same time, the kinematic and dynamic constraints of the Bunkerpro unmanned ground vehicle must be satisfied. Unlike traditional path planning methods that simplify the UGV to a particle model, this study takes more key factors into account, such as the platform's size and LiDAR placement height, in order to overcome the shortcomings of traditional methods that overlook motion constraints and environmental factors.

4.2.1 Model preparation

In practical applications, data collection usually relies on existing Building Information Models (BIM) to obtain relevant information about construction sites. Given this, the study selected a classroom and corridor model from the fifth floor of the Engineering Building at university campus for path planning. As shown in Figure 7, the classroom model contains many obstacles (such as desks, chairs, and podiums), which is similar to the noisy environment of a construction site. The corridor model has a large coordinate range and a high point cloud density, which is similar to the point cloud data scale encountered in real construction sites. Both models are ideal choices for validating path planning and simulating LiDAR scanning effects.

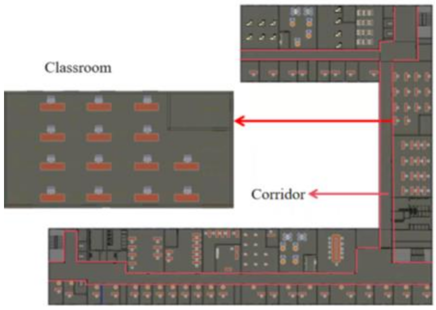

Figure 7. BIM models of classroom and corridor

In this study, the total number of points generated for the corridor and classroom models was set to 100,000, with the point cloud density set to 10 to ensure the preservation of model details. The generated point cloud models required further adjustments to ensure their dimensions and coordinates aligned with the actual building. To achieve this, the researchers imported the models into 3ds Max to adjust their coordinates and dimensions. The final result is shown in Figure 8.

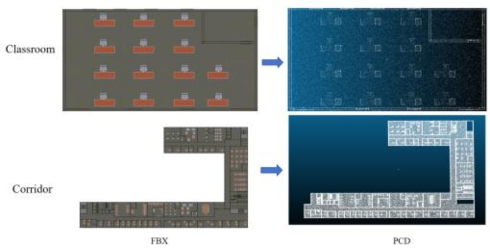

Figure 8. BIM models of classroom and corridor

4.2.2 Algorithm results

This algorithm aims to simulate data collection by an UGV equipped with LiDAR along a planned path. Due to the relatively small passable areas in the two models, the researchers set the grid coordinates to the size of the UGV (0.9m) to ensure smooth passage. The cloud-to-cloud algorithm was used to calculate the ground point cloud thickness of the model as 0.2m. In the algorithm, the parts at an elevation of 0.2m were designated as the ground for the UGV, and a feasible path map was generated (as shown in Figure 9). In addition, to ensure that the path does not collide with obstacles and that the start and end points are within valid areas, the constraint equations are used as follows:

$$g_1(x) = valid\_path(x) = Ture \quad (1)$$

$$g_2(x) = start\_point\_valid(x) = Ture \quad (2)$$

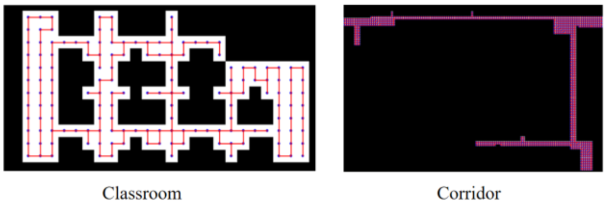

Figure 9. Feasible path map of classroom and corridor

It is important to note that during this process, the LiDAR simulates emitting rays within a specific angular range and checks where each ray intersects with the point cloud. In this study, the parameters of the Livox Mid-360 were used to set the LiDAR's field of view (fov=360°), scanning angle range (up_angle=52°, down_angle=7°), mounting height (h=0.7m), and measurement range (range_min=0.1m, range_max=70m). The rays are traced in each direction until they hit the nearest point in the point cloud. This setup ensures that the system does not detect point clouds behind obstacles, thus reducing noise interference.

In this algorithm, the objective function can be the number of point clouds covered by the path, that is, the number of valid point clouds scanned in the area traversed by the path. This reflects the optimization effect of the path and is defined as:

$$f_{objective}(\mathrm{x}) = \mathrm{coverage}(\mathrm{x}) \quad (3)$$

The researchers recorded the number of point clouds corresponding to the optimal path in each generation (as shown in Figure 10). During the simulation scanning process in the tenth generation of GA, the maximum number of point clouds was obtained, with values of 6115 and 30606, respectively. As shown in Line charts, the point cloud collection gradually stabilized in the later generations for both models. This indicates that the GA converged after several generations of optimization, and the model's performance became consistent. The number of point clouds collected reached the optimal state during the optimization process, confirming the success of the framework in this study. Furthermore, it is important to note that in GA's iterative process, it is possible for two generations to produce identical results. This happens because the fitness function of the offspring, after crossover and mutation, is lower than the optimal result of the parent generation.

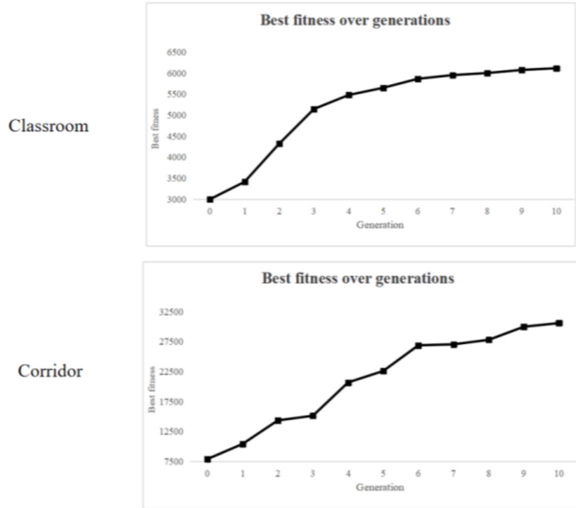

Figure 10. Convergence trends of GA

Figure 11 shows the coordinate information of the paths for the two models and the preview of the point cloud. The coordinate information of the path reflects the specific distribution of the optimal solution after optimization by GA in the coordinate space, while the point cloud preview displays the distribution of the point cloud data collected along the optimized path, providing a clear and intuitive reference.

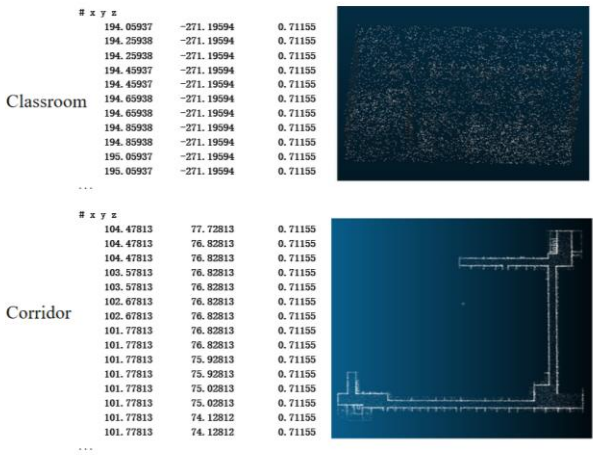

Figure 11. Path coordinate set and simulation models

Through approximate calculation, the longest path is 1417.09m and the shortest is 1203.32m. From the Figure 12, it can be seen that the path length does not show an obvious pattern of change and does not exhibit a significant convergence trend. Among them, the third-generation path, due to random variations, shows a significantly longer result compared to other generations. It can be attributed to the exploratory nature of the algorithm in the early stages of evolution, which is a common occurrence in the initial phase of GA optimization.

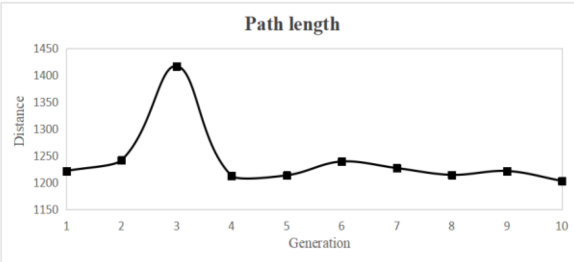

Figure 12. Changes in path length per generation

4.2.3 Data normalization

For point cloud path planning and scanning coverage optimization, the goal of data normalization is to bring different evaluation metrics to a unified dimension, allowing researchers to derive an optimal path based on the scoring rules they formulated.

Since the classroom model is relatively small, path length is not considered as a scoring factor for its optimal path. For the corridor model, researchers selected point cloud quantity and path length as scoring metrics, assigning weights of 80% and 20%, respectively. Path length, being a common optimization objective, means that shorter paths result in lower task costs (such as collection time, battery consumption of the autonomous vehicle, etc.).

The normalized calculation results and final scores are shown in Table 2, with the tenth generation path receiving the highest score. This indicates that the path in the tenth generation achieved the best balance during the optimization process, representing the optimal trade-off between path length and point cloud coverage. Therefore, the path from the tenth generation was selected as the optimal result for this experiment and output as the final recommended path.

Table 2. Scoring results for all paths

Generation	Best Fitness	Path length	Score
1	0.111	0.914	0.272
2	0.284	0.820	0.391
3	0.319	0.000	0.255
4	0.563	0.956	0.642
5	0.648	0.951	0.709
6	0.837	0.831	0.836
7	0.844	0.888	0.853
8	0.877	0.947	0.891
9	0.973	0.914	0.961
10	1.000	1.000	1.000

5 Discussion

This study first converted the BIM model of the fifth-floor corridor and classroom of the Engineering Building into a point cloud model. During this process, software limitations caused coordinate system confusion, requiring researchers to adjust coordinates and obstacle dimensions comprehensively using professional 3D modeling software.

Next, a path optimization algorithm (combining GA and A* algorithm) was developed in Python to maximize data collection by UGVs in three-dimensional space. The algorithm iteratively searched for the optimal path over multiple generations, eventually converging to the best path planning scheme, ensuring that the LiDAR covered all target areas as comprehensively as possible. Notably, the algorithm allows researchers to select the most suitable path based on specific needs. In the tenth generation of GA, path optimization reached its optimal state according to the weighted scoring system.

The experimental results indicate that during the path optimization process, the number of scanned point clouds increases continuously and eventually stabilizes. Researchers can flexibly choose the path from the stable results based on different experimental requirements.

Moreover, It is worth noting that the algorithm has certain CPU performance requirements and relatively low precision requirements for imported point cloud data, retaining only the essential key details. In practical applications, to improve efficiency and save time, it is recommended to limit the size of point cloud data to within 100 MB to meet practical needs while ensuring the high efficiency of the algorithm.

6 Conclusion

This study proposes an innovative path planning method that ensures UGVs can capture point cloud data more comprehensively in noisy construction environments, thereby improving model completeness. Additionally, by overcoming the limitations of existing tools, we elevate radar scanning simulation from the traditional 2D (such as the MATLAB Driving Scenario Designer) to 3D, and accurately track and record the spatial areas that can be captured within the scan range.

Experimental results show that this path planning method exhibits high adaptability, allowing adjustments based on different laser radar performance characteristics (such as scanning range and installation position). Moreover, the algorithm iteratively optimizes the path to minimize scanning blind spots, enhancing the coverage of the laser radar and consequently obtaining denser point cloud data, providing a more comprehensive data foundation for building inspections.

References

[1] Halder S, Afsari K. Robots in Inspection and Monitoring of Buildings and Infrastructure: A Systematic Review. Applied Sciences. 2023;13(4):2304.

[2] Hallermann N, Morgenthal G, Rodehorst V. Unmanned Aerial Systems (UAS) – Case Studies of Vision Based Monitoring of Ageing Structures2015.

[3] Pinto L, Bianchini F, Nova V, Passoni D. Low-Cost UAS Photogrammetry for Road Infrastructures' Inspection ISPRS - International Archives of the Photogrammetry, Remote Sensing and Spatial Information Sciences. 2020;XLIII-B2-2020:1145-50.

[4] Jiashen S. Exploring the influence and importance of engineering testing on quality control of construction projects. Engineering Management and Technical Discussion. 2022;4(16).

[5] Cong C. Brief Analysis of the Characteristics and Methods of Construction Engineering Inspection. Engineering Construction Technology. 2023;1(5):23-5.

[6] Lattanzi D, Miller G. Review of Robotic Infrastructure Inspection Systems. Journal of Infrastructure Systems. 2017;23:04017004.

[7] Asadi K, Jain R, Qin Z, Sun M, Noghabaei M, Cole J, et al. Vision-Based Obstacle Removal System for Autonomous Ground Vehicles Using a Robotic Arm2019. 328-35 p.

[8] Wang X, Pan H, Guo K, Yang X, Luo S. The evolution of LiDAR and its application in high precision measurement. IOP Conference Series: Earth and Environmental Science. 2020;502:012008.

[9] Ilyas M, Ying K, Nithish M, Xin J, Xinge Z, Cheah C. Robot-Assisted Object Detection for Construction Automation: Data and Information-Driven Approach. IEEE/ASME Transactions on Mechatronics. 2021;PP:1-.

[10] Kau L-J, Chiou L-J, Lo Y-H, Chen S-H. A Multi-Lidar-based Point Cloud Acquisition Platform and Data Fusion for Autonomous Vehicle in Complex Urban Environment2023. 1-5 p.

[11] Nolan P, Paley D, Kroeger K. Multi-UAS path planning for non-uniform data collection in precision agriculture2017. 1-12 p.

[12] Popovic M, Vidal-Calleja T, Hitz G, Chung J, Sa I, Siegwart R, et al. An informative path planning framework for UAV-based terrain monitoring. Autonomous Robots. 2020;44.

[13] Pan Y, Yang Y, Li W. A Deep Learning Trained by Genetic Algorithm to Improve the Efficiency of Path Planning for Data Collection With Multi-UAV. IEEE Access. 2021;PP:1-.

[14] Hua X. Research on path planning and motion control of unmanned platforms under unstructured roads [D]. Jilin: Jilin University; 2023.

[15] Wang S, Li A. Multi-adjacent-vertexes and Multi-shortest-paths Problem of Dijkstra Algorithm. Computer Science. 2014;41(6):217-24.

[16] Wang M. Mobile robot path planning based on A* algorithm [D]. Shenyang: Shenyang University of Technology; 2017.

[17] Baker ZK, Gokhale M, editors. On the Acceleration of Shortest Path Calculations in Transportation Networks. 15th Annual IEEE Symposium on Field-Programmable Custom Computing Machines (FCCM 2007); 2007 23-25 April 2007.

[18] Wang P, Liu Y, Yao W, Yu Y. Improved A-star algorithm based on multivariate fusion heuristic function for autonomous driving path planning. Proceedings of the Institution of Mechanical Engineers, Part D: Journal of Automobile Engineering. 2022;237:095440702211006.

[19] Bao W, Li J, Pan Z, Yu R. Improved A-star Algorithm for Mobile Robot Path Planning Based on Sixteen-direction Search2022. 1332-6 p.

[20] Nguyen HT, Le HX. Path planning and Obstacle avoidance approaches for Mobile robot. ArXiv. 2016;abs/1609.01935.

[21] Dong Y, Cao J, Li G. Automatic Guided Vehicle Path Planning Based on A-Star and DWA Dual Optimization Algorithms. Science Technology and Engineering. 2023;23(30):12994-3001.

[22] Baras N, Dasygenis M. UGV Coverage Path Planning: An Energy-Efficient Approach through Turn Reduction. Electronics. 2023;12(13):2959.

[23] Lo Y, Cao Y, Zhou X, Zhang C, Chen M. Performance Analysis of Low-Cost Solid-State LiDAR for Building Elements Point-Cloud Mapping. ICiMR 2024; 22-23 August 2024, Taicang, China.